

## Thermally stimulated current transport peaks in insulating layers with spatially non-homogeneous trap distribution

This article has been downloaded from IOPscience. Please scroll down to see the full text article.

1990 J. Phys.: Condens. Matter 2 3311

(<http://iopscience.iop.org/0953-8984/2/14/015>)

View [the table of contents for this issue](#), or go to the [journal homepage](#) for more

Download details:

IP Address: 171.66.16.96

The article was downloaded on 10/05/2010 at 22:00

Please note that [terms and conditions apply](#).

## Thermally stimulated current transport peaks in insulating layers with spatially non-homogeneous trap distribution

W Tomaszewicz†, J Rybicki, B Jachym†, M Chybicki and S Feliziani‡  
Faculty of Technical Physics and Applied Mathematics, Technical University of Gdańsk,  
Majakowskiego 11/12, 80-952 Gdańsk, Poland

Received 11 April 1989

**Abstract.** In the present work we have investigated the influence of spatial non-homogeneity of trap distribution on thermally stimulated currents (TSC) due to transport of carriers in insulating layers. It has been assumed that at zero time carriers are generated only in a thin layer near one of the contacts. We have proved that for both non-dispersive and dispersive transport the initial increase of TSC is strongly dependent on the spatial distribution of traps. On the other hand, the dependence of TSC maximum on electric field strength, layer thickness and heating rate, and in the case of dispersive transport also on the final current decay, is almost the same as for a homogeneous trap distribution. The analytical results have been found to agree satisfactorily with the results of Monte Carlo simulation of non-isothermal carrier transport for all the model spatial and energetic trap distributions considered. The possibility of determining spatial trap distribution on the basis of the measured TSC has been discussed.

### 1. Introduction

In the transport of charge carriers in insulators and semiconductors, the dominant role is often played by localised states (traps) in the forbidden gap. Fundamental progress in the theoretical description of dispersive transient currents, characteristic of many amorphous materials, has been made by Scher and Montroll (1975), Noolandi (1977a, b) and Schmidlin (1977) (later works are quoted in excellent review papers by Pfister and Scher (1978) and Marshall (1983)). The theory has been generalised to the case of non-isothermal transient currents (Samoć and Samoć 1980, Plans *et al* 1981, 1983, Tomaszewicz and Jachym 1984, Schrader and Kryszewski 1985, Tomaszewicz 1985).

In all the works quoted, however, only a spatially homogeneous trap distribution has been considered. The assumption of spatial homogeneity of trap concentration is unjustified for very thin layers, where regions of near-surface non-homogeneity are comparable with the layer thickness. Current-time characteristics may then differ remarkably from those for a homogeneous trap distribution (Samoć and Zboiński 1978). The influence of spatial non-uniformity of trap density on multiple-trapping transient

† Also at: Laboratory of Organic Dielectrics and Semiconductors, Technical University of Gdańsk, Majakowskiego 11/12, 80-952 Gdańsk, Poland.

‡ Also at: Istituto di Matematica e Fisica, Università di Camerino, Camerino, Italy.

currents in the case of isothermal transport has been considered by Rybicki and Chybicki (1988, 1989). In the present work we describe analogous results for non-isothermal transport. Section 2 presents the analytical solution of transport equations, which are compared to the results of the Monte Carlo simulation in section 3. The possibility of determining the spatial trap distribution on the basis of measured thermally stimulated currents (TSC) is discussed in section 4. Section 5 contains concluding remarks.

## 2. Analytical considerations

### 2.1. Transport equations

The system of equations describing non-isothermal multiple-trapping transport of carriers in layers with spatially non-homogeneous trap distribution may be written as the following generalisation of transport equations formulated by Plans *et al* (1981):

$$\frac{\partial}{\partial t} [n(x, t) + n_t(x, t)] + \mu_0 E \frac{\partial n(x, t)}{\partial x} = 0 \quad (1)$$

$$\frac{\partial n'_t(x, t, \mathcal{E})}{\partial t} = C_t N_t(x, \mathcal{E}) n(x, t) - \frac{n'_t(x, t, \mathcal{E})}{\tau_d(t, \mathcal{E})} \quad (2)$$

where  $x$  is spatial coordinate ( $0 \leq x \leq L$ ),  $t$  is time ( $t \geq 0$ ),  $\mathcal{E}$  is depth of trap (measured down from the bottom of the conduction band),  $n(x, t)$  and  $n_t(x, t)$  are concentrations of free and trapped carriers, respectively,  $n'_t(x, t, \mathcal{E})$  and  $N_t(x, \mathcal{E})$  are concentrations of trapped carriers and traps per unit energy,  $\tau_d(t, \mathcal{E})$  is mean detrapping time at time  $t$  from the trap of depth  $\mathcal{E}$ ,  $\mu_0$  is microscopic mobility of carriers,  $E$  is external electric field applied to the layer and  $C_t$  is capture coefficient. Equations (1) and (2) are the continuity equation and the trapping–detrapping kinetics equation, respectively. The trap density  $N_t(x, \mathcal{E})$  may be written as

$$N_t(x, \mathcal{E}) = S(x)N(\mathcal{E}) \quad (3)$$

where the functions  $S(x)$  (dimensionless) and  $N(\mathcal{E})$  describe spatial and energetic trap distributions, respectively. The mean detrapping time  $\tau_d(t, \mathcal{E})$  is given by

$$\tau_d(t, \mathcal{E}) = \nu_0^{-1} \exp[\mathcal{E}/kT(t)] \quad (4)$$

where  $\nu_0$  is a frequency factor,  $k$  is Boltzmann's constant and  $T(t)$  is temperature of the layer at time  $t$ . The main simplifying assumptions under which equations (1)–(4) are valid are: neglect of diffusion and space-charge effects; small trap occupation; and temperature independence of  $\mu_0$ ,  $C_t$  and  $\nu_0$ .

Integrating (2) with the initial condition  $n'_t(x, 0, \mathcal{E}) = 0$  (at initial time  $t = 0$  there are no trapped carriers in the layer), one obtains the following relation between the concentrations of trapped and free carriers:

$$n_t(x, t) = S(x) \int_0^t \Phi(t, t') n(x, t') dt' \quad (5)$$

where function  $\Phi(t, t')$  is given by

$$\Phi(t, t') = C_t \int_{\mathcal{E}_t^0}^{\mathcal{E}_t} N(\mathcal{E}) \exp\left(-\int_{t'}^t \frac{dt''}{\tau_d(t'', \mathcal{E})}\right) d\mathcal{E} \quad (6)$$

and  $\mathcal{E}_t^0$  and  $\mathcal{E}_t$  are limits of the energetic trap distribution.

The current induced in the measurement circuit by the carrier motion is given by

$$I(t) = \frac{I_0}{n_0 L} \int_0^L n(x, t) dx \quad (7)$$

where  $I_0 = en_0\mu_0EA$ ,  $e$  is elementary charge,  $n_0$  is concentration of initially generated carriers, averaged over the layer thickness  $L$ , and  $A$  is contact surface. In the initial stages of transport, when the density of free carriers on the collecting electrode is negligible ( $n(L, t) \approx 0$ ), the current intensity  $I(t)$  may be expressed as (cf Schrader and Kryszewski 1985)

$$I(t) \approx \frac{I_0}{\mu_0 E} \frac{d\bar{x}(t)}{dt} \quad (8)$$

where  $\bar{x}(t)$  describes the motion of the carriers' centroid

$$\bar{x}(t) = \frac{1}{n_0 L} \int_0^L x[n(x, t) + n_t(x, t)] dx. \quad (9)$$

## 2.2. Relation to equations for homogeneous trap density

We shall assume the following inequalities to be fulfilled:  $n(x, t) \ll n_t(x, t)$  and  $\partial n(x, t)/\partial t \ll \partial n_t(x, t)/\partial t$ . In the case of a homogeneous spatial trap distribution it may be shown that the above inequalities are valid for  $t \gg \tau_0$ , where  $\tau_0 = L/\mu_0 E$  is the trap-free time of flight (Tomaszewicz and Jachym 1984). It may be expected that an analogous situation also occurs in non-homogeneous layers.

Under those assumptions a simple relation between carrier transport in homogeneous and non-homogeneous layers may be found. Introducing a new spatial coordinate

$$z(x) = \frac{1}{\mu_0 E} \int_0^x S(x') dx' \quad (10)$$

and new notations  $\bar{n}(z(x), t) = n(x, t)$ ,  $\bar{n}_t(z(x), t) = n_t(x, t)/S(x)$ , equations (1) and (5) assume identical form as in the case of the homogeneous trap distribution (Tomaszewicz and Jachym 1984):

$$\frac{\partial \bar{n}_t(z, t)}{\partial t} + \frac{\partial \bar{n}(z, t)}{\partial z} \approx 0 \quad (11)$$

$$\bar{n}_t(z, t) = \int_0^t \Phi(t, t') \bar{n}(z, t') dt' \quad (12)$$

which implies that the solutions obtained previously for the homogeneous trap distribution may be easily adopted for the non-homogeneous trap distribution case. In the following we confine ourselves to the situation in which the carriers are initially generated in an infinitesimally thin layer in  $x = 0$ .

## 2.3. Non-dispersive transport

Non-dispersive transport occurs when the carriers in the conduction band and in traps are in thermal quasi-equilibrium. Equation (12), which describes trapping–detraping

kinetics, may then be replaced by an approximate equation (Tomaszewicz and Jachym 1984)

$$\bar{n}_t(z, t) \approx \bar{n}(z, t)/\theta(t) \quad (13)$$

where the function  $\theta(t)$  is given by

$$\theta^{-1}(t) = C_t \int_{\mathcal{E}^0}^{\mathcal{E}_t} N(\mathcal{E}) \tau_d(t, \mathcal{E}) d\mathcal{E}. \quad (14)$$

As will be seen from subsequent equations, approximation (13) ignores broadening of the carrier packet. In fact, carrier transport under conditions of thermal quasi-equilibrium may be proved to be Gaussian in homogeneous layers (Tomaszewicz 1985). However, carrier dispersion, when included in the equations, does not change the following results significantly.

Equation (11) can now be solved to give

$$\bar{n}(z, t) = n_0 L \theta(t) \delta[z - \zeta(t)] \quad (15)$$

where  $\delta$  is the Dirac function, and

$$\zeta(t) = \int_0^t \theta(t') dt'. \quad (16)$$

Returning to the original variables and using the properties of the  $\delta$  function one gets

$$n(x, t) = \frac{n_0 L \theta(t)}{S[\bar{x}(t)]} \delta[x - \bar{x}(t)] \quad (17)$$

$$n_t(x, t) = n_0 L \delta[x - \bar{x}(t)] \quad (18)$$

where the position of a carrier packet is given by  $z[\bar{x}(t)] = \zeta(t)$ , which explicitly reads

$$\int_0^{\bar{x}(t)} S(x) dx = \mu_0 E \zeta(t). \quad (19)$$

The time dependence of TSC, according to (7) or (8), is given by

$$I(t) = \frac{I_0 \theta(t)}{S[\bar{x}(t)]} H[L - \bar{x}(t)] \quad (20)$$

where  $H$  is the unit step function. As is easily seen, the TSC depends distinctly on the spatial trap distribution, being inversely proportional to the local trap density. According to equation (20) the TSC decays immediately at the moment  $\tau_e$ , corresponding to the effective carrier time of flight;  $\tau_e$  is given by  $\bar{x}(\tau_e) = L$ , which with the aid of (19) may be written as

$$\zeta(\tau_e) = \tau_0 S_{av} \quad (21)$$

where  $S_{av}$  is the mean value of  $S(x)$ :

$$S_{av} = \frac{1}{L} \int_0^L S(x) dx. \quad (22)$$

According to equation (21), the time of flight  $\tau_e$  is an increasing function of the ratio  $L/E$ , and depends only on the manner and rate of heating, that is on the form of the

function  $T(t)$ , and on  $S_{av}$  given by (22). In particular,  $\tau_e$  does not depend on the specific form of the spatial trap distribution  $S(x)$ .

2.4. Dispersive transport

In the case of dispersive transport, equation (12) relating trapped- and free-carrier concentrations, may be replaced by the approximate formula (Tomaszewicz and Jachym 1984)

$$\frac{\partial}{\partial t} \left( \frac{\bar{n}_t(z, t)}{\Phi(t, 0)} \right) = \bar{n}(z, t). \tag{23}$$

In what follows we shall simply write  $\Phi(t)$  instead of  $\Phi(t, 0)$ . In the case of dispersive transport  $\Phi(t)$  may be given by the approximate expression

$$\Phi(t) = C_t \int_{\mathcal{E}_0(t)}^{\mathcal{E}_t} N(\mathcal{E}) d\mathcal{E} \tag{24}$$

where demarcation level  $\mathcal{E}_0(t)$  is given by the equation

$$\int_0^t \frac{dt'}{\tau_d[t', \mathcal{E}_0(t)]} = 1. \tag{25}$$

The demarcation level  $\mathcal{E}_0(t)$  splits traps into those which reached equilibrium occupation and those from which there was practically no release up to time  $t$ .

Equation (11) with the aid of (23) solves to give

$$\bar{n}_t(z, t) = n_0 \tau_0 \Phi(t) \exp[-z\Phi(t)]. \tag{26}$$

Returning to the original variables one gets from equations (23) and (26)

$$n(x, t) = n_0 \tau_0 \frac{d}{dt} \{ \exp[-z(x)\Phi(t)] \} \tag{27}$$

$$n_t(x, t) = n_0 \tau_0 \Phi(t) S(x) \exp[-z(x)\Phi(t)]. \tag{28}$$

The intensity of the TSC, according to (7), is given by

$$I(t) = \frac{I_0}{\mu_0 E} \frac{d}{dt} \int_0^L \exp[-z(x)\Phi(t)] dx. \tag{29}$$

The integral in the last expression cannot be calculated analytically for an arbitrary spatial trap distribution. However, in the following two limiting cases approximate formulae may be developed.

Let us assume first that  $z(L)\Phi(t) = \tau_0 S_{av} \Phi(t) \gg 1$ . The exponential function in the integrand in (29) may then be replaced by the unit step function  $H[\bar{x}(t) - x]$ , where the function  $\bar{x}(t)$  is given by  $z[\bar{x}(t)]\Phi(t) = 1$ , that is by

$$\int_0^{\bar{x}(t)} S(x) dx = \mu_0 E / \Phi(t). \tag{30}$$

The intensity of the TSC is now

$$I(t) \approx \frac{I_0}{S[\bar{x}(t)]} \frac{d}{dt} \left( \frac{1}{\Phi(t)} \right). \tag{31}$$

Equation (31) results also from (8) and (30), which means that the function  $\bar{x}(t)$  describes

approximately the motion of the drifting carriers' centroid. Provided the function  $S(x)$  does not increase too rapidly with  $x$ , equation (31) corresponds to the TSC increase. The TSC maximum should occur in a time close to the time of flight  $\tau_e$ ;  $\tau_e$  is given by the equation  $\bar{x}(\tau_e) = L$ , which, as results from (30), is equivalent to

$$\tau_0 S_{av} \Phi(\tau_e) \approx 1. \quad (32)$$

Because  $\Phi(t)$  decreases monotonically in time, equation (31) is valid for times  $t \ll \tau_e$ . It may be noted that equations (30)–(32) are analogous to equations (19)–(21) for non-dispersive transport. Similarly as in the case of non-dispersive transport, the initial TSC increase depends distinctly on the spatial trap distribution (equation (31)), whereas the latter only weakly influences the dependences of the position of the TSC maximum on applied electric field, layer thickness and manner and rate of heating (equation (32)).

Let us now consider the second limiting case:  $\tau_0 S_{av} \Phi(t) \ll 1$ , which is valid for  $t \gg \tau_e$ . The exponential function in the integrand of (29) may then be developed into a power series. Retaining the first two terms one gets

$$I(t) \approx CI_0 \tau_0^2 [-d\Phi(t)/dt] \quad (33)$$

where

$$C = \frac{1}{L^2} \int_0^L (L-x)S(x) dx. \quad (34)$$

As is easily seen, the spatial trap distribution does not influence the shape of the final decay of the TSC, despite the presence of the multiplicative constant  $C$ .

### 3. Numerical results and discussion

Up till now neither the manner of heating nor the energetic and spatial distributions of traps have been specified. In order to calculate illustrative TSC curves we shall assume the linear heating scheme  $T(t) = T_0 + \beta t$ , where  $T_0$  is the initial temperature of the sample and  $\beta$  is the heating rate. As far as the energetic trap distribution is concerned, we shall use the discrete single level

$$N(\mathcal{E}) = N_0 \delta(\mathcal{E} - \mathcal{E}_0) \quad (35)$$

for non-dispersive transport ( $\mathcal{E}_0$  is trap depth), and the exponential distribution

$$N(\mathcal{E}) = \frac{N_0}{kT_c} \exp\left(-\frac{(\mathcal{E} - \mathcal{E}_t^0)}{kT_c}\right) \quad (36)$$

for dispersive transport. In equation (36)  $T_c$  is the characteristic temperature of the energetic trap distribution,  $\mathcal{E}_t^0$  is the upper edge of the distribution and  $N_0$  is chosen in such a way that the product  $N_0 S(x)$  is the total trap concentration in  $x$ . The model spatial trap distributions are chosen to be

$$S(x) = \exp(-x/D) \quad (37)$$

and

$$S(x) = \exp[-(L-x)/D]. \quad (38)$$

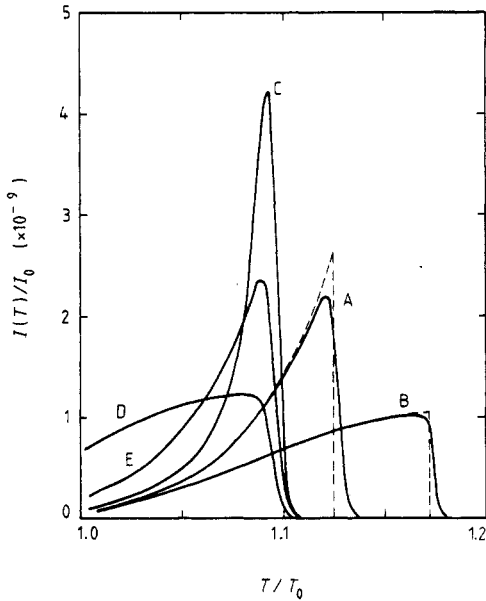


**Figure 1.** Non-dispersive TSC curves for a non-homogeneous spatial trap distribution and linear heating. Full curves correspond to Monte Carlo simulation; broken curves correspond to approximate solutions (19) and (20). Curves: A, trap distribution (37) with  $L/D = 0$  (homogeneous trap distribution); B,  $L/D = -2$ ; C,  $L/D = 2$ ; D, trap distribution (38),  $L/D = 2$ ; E, homogeneous trap distribution with the same mean trap density as for C and D. Here  $\tau_0\beta/T_0 = 10^{-10}$ ,  $\tau(x)S(x)\beta/T_0 = 2 \times 10^{-13}$ ,  $\nu_0 T_0/\beta = 5 \times 10^{15}$ ,  $\xi_0/kT_0 = 30$ .

Full curves in figure 1 show the non-dispersive TSC curves calculated with the aid of the Monte Carlo simulation, performed according to the algorithm described by Tomaszewicz (1988), which is the generalisation of the procedure used for the isothermal case, e.g. by Marshall (1977). The procedure consists of choosing repeatedly a random value of the free-carrier lifetime  $\tau^r(x)$  according to the equation

$$\tau^r(x) = -\tau(x) \ln X \tag{39}$$

where  $\tau(x)$  is the mean trapping time in  $x$ , and a random value of the detrapping time  $\tau_d^r(t)$ , which is the solution of the equation

$$\nu_0 \int_t^{t+\tau_d^r} \exp\left(-\frac{\xi_t}{kT(t')}\right) dt' = -\ln Y \tag{40}$$

where  $X$  and  $Y$  are random numbers from the interval  $(0, 1)$ , and  $t$  is the moment of carrier capture. The free-carrier displacement and the resulting current in the external circuit are given by  $\Delta x = L\tau^r(x)/\tau_0$  and  $\Delta I = e/\tau_0$ . The Monte Carlo results have been obtained from averaging over  $10^5$  carriers.

The approximate solution (19)–(20) has been plotted using the broken curve (only for curves A and B in order not to complicate the figure). The discrepancies between the Monte Carlo results and the approximate solution occur entirely for times close to  $T_e$ , where the temperature  $T_e = T(\tau_e)$  corresponds to the current maximum.

Curve A in figure 1 corresponds to the homogeneous trap density  $N_0$ , and curves B and C to the trap density increasing and decreasing exponentially in  $x$  from the same trap concentration in  $x = 0$ . The differences in the position of the TSC peak height are attributed to different numbers of traps in the layer. The differences in the shapes of the calculated TSC curves are due to different spatial trap distributions. This dependence is more apparent if one compares the TSC calculated for different spatial trap distributions, the total number of traps in the layer being constant (curves C–E in figure 1). Thus curves C and D illustrate a strong polarity dependence of TSC in non-homogeneous



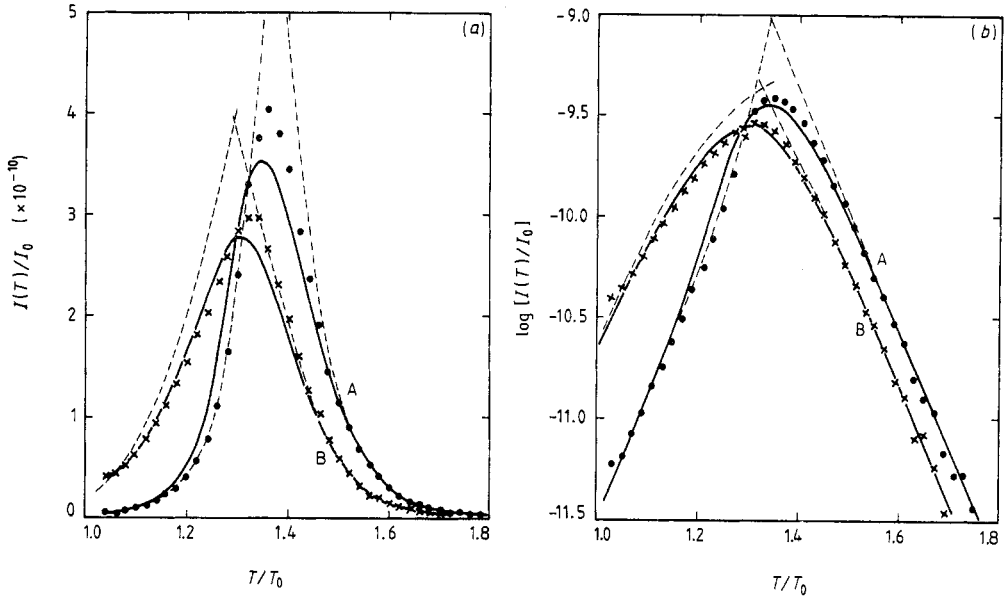


**Figure 2.** (a) Dispersive TSC curves for non-homogeneous spatial trap distribution and linear heating,  $T/T_c = 0.33$ . Curves: A, trap distribution (37),  $L/D = 2$ ; B, trap distribution (38),  $L/D = 2$ . Circles and crosses are Monte Carlo simulation; full curves are calculations on the basis of equations (10), (24), (25) and (29); broken curves correspond to current increase and decrease according to equations (31) and (33)–(34), respectively. Here  $\tau_0\beta/T_0 = 10^{-10}$ ,  $\tau(x)S(x)\beta/T_0 = 1.187 \times 10^{-13}$ ,  $\nu_0 T_0/\beta = 10^{15}$ . (b) The same as (a) but on a semi-logarithmic scale.

layers. For comparison, the current for traps distributed uniformly in space with the same mean concentration has also been shown (curve E).

Figures 2 and 3 show typical TSC curves in the case of dispersive transport for two different values of the characteristic temperature  $T_c$ . Full curves have been calculated on the basis of equations (10), (24), (25) and (29) for the trap density decreasing and increasing exponentially in  $x$ , with the same maximum trap density. The numerical results have again been compared with the Monte Carlo simulation, where to describe each trapping–detrapping event a third random value—the trap depth  $\mathcal{E}_t^{\dagger}$ —was chosen according to the equation

$$\int_{\mathcal{E}_t^{\dagger}}^{\mathcal{E}_t^{\ddagger}} \frac{N_t(\mathcal{E})}{N_0} d\mathcal{E} = Z \quad (41)$$

where  $Z$  is a random number from the interval  $(0, 1)$ . The Monte Carlo results are shown in figures 2 and 3 with circles and crosses. The discrepancies between the Monte Carlo results and the analytical formulae obtained should be attributed to the approximations made in the development of equation (29). In general, the analytical solutions reproduce well the Monte Carlo results in the case of strongly dispersive transport ( $T/T_c \leq 0.2$ ). Broken curves in figures 2 and 3 correspond to the approximate expressions for the initial current increase and the final current decay (equations (31) and (33)–(34), respectively). They agree quite well with equation (29) for the homogeneous trap distribution.

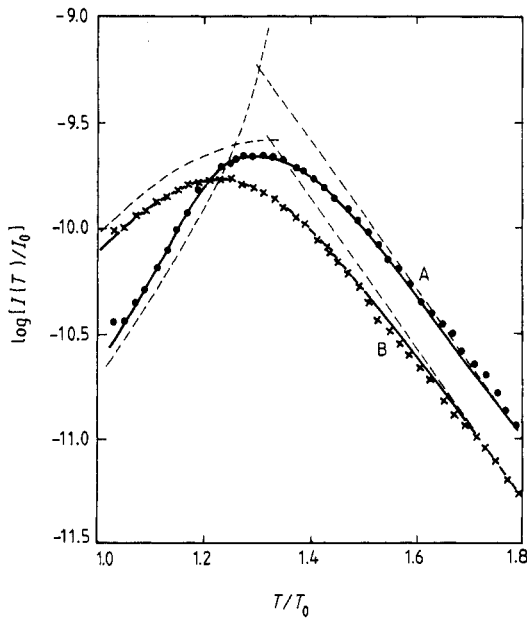


**Figure 3.** Dispersive TSC curves for non-homogeneous spatial trap distribution and linear heating,  $T/T_c = 0.2$ . Curves: A, trap distribution (37),  $L/D = 2$ ; B, trap distribution (38),  $L/D = 2$ . The meaning of curves and the values of other parameters are as in figure 2.

However, the discrepancies grow with increasing degree of spatial non-homogeneity of the trap distribution.

#### 4. Methods for determining spatial trap distribution

As has been shown in the previous sections, the full course of TSC depends on the energetic and spatial trap distributions. The latter does not have any significant influence on the dependence of the position of the TSC peak on the field intensity, sample thickness or heating manner and rate. In the case of dispersive transport, the spatial trap distribution also has practically no influence on the shape of the final TSC decay. On this basis, the quantities describing the energetic trap distribution can be determined in exactly the same way as the ones used for traps uniformly distributed in the sample bulk (Samoć and Samoć 1980, Plans *et al* 1981, Tomaszewicz and Jachym 1984, Schrader and Kryszewski 1985, Tomaszewicz 1985). Next, from equations (20) or (31) the shape function  $S(x)$ , characterising the spatial trap distribution, can be determined. In the following we shall illustrate it with the examples of energetic trap distributions (35) and (36), for non-dispersive and dispersive transport, respectively, as well as a linear heating scheme.

For non-dispersive transport, from equations (20) and (21) one gets

$$I(T) \sim \frac{\exp(-\mathcal{E}_t/kT)}{S(\bar{x}(T))} \quad (42)$$

$$T_c^{-1} \approx \frac{k}{\mathcal{E}_t} \ln\left(\frac{c_1 E}{\beta L}\right) \quad (43)$$

where the constant  $c_1$  depends on the trap parameters and the free-carrier mobility  $\mu_0$ .

It is clear that, after determining the trap depth  $\mathcal{E}_t$  on the basis of the dependence (43), it is possible, using equation (42), to determine also the shape function  $S(\bar{x}(T))$ . As follows from equation (8), the charge  $Q(T)$ , collected till the sample temperature reaches  $T$ , is expressed by the Ramo theorem (Ramo 1939):

$$Q(T) = Q_0 \bar{x}(T)/L \quad (44)$$

where  $Q_0 = I_0 \tau$  is the total charge of carriers generated in the sample. Charge  $Q_0$  corresponds to the area under the TSC curve, while charge  $Q(T)$  corresponds to the part of this area to the left of the point  $T$ . The last formula allows the determination of the position of the carrier centroid as a function of temperature, and thus the determination of the shape of the spatial trap distribution.

Let us now consider dispersive transport. For a linear heating scheme, the demarcation level  $\mathcal{E}_0(T)$ , defined by equation (25), is described by the approximate expression  $\mathcal{E}_0(T) \approx k(c^*T - T^*)$ , where  $c^*$  depends on the frequency factor and the sample's heating rate (Tomaszewicz and Jachym 1984). Then from equations (31)–(34) we have

$$I(T) \sim \frac{\exp(c^*T/T_c)}{S(\bar{x}(T))} \quad \text{for } T < T_e \quad (45)$$

$$T_e = \frac{T_c}{c^*} \ln\left(\frac{c_2 L}{E}\right) \quad (46)$$

$$T(t) \sim \exp(-c^*T/T_c) \quad \text{for } T > T_e \quad (47)$$

where constant  $c_2$  depends on trap parameters and carrier mobility  $\mu$ . It can be seen that after determining the ratio  $c^*/T_c$  from the dependence (46) or (47), one can, in principle, obtain the shape of the trap distribution on the basis of equations (45) and (44) in a manner analogous to that used for non-dispersive transport. However, it must be remembered that equation (31), from which (45) follows, is satisfactorily exact only for a slowly changing function  $S(x)$ . In the general case, formula (29) may be applied to determine the spatial trap distribution. It requires calculating the shape of function  $\Phi(t)$  on the basis of the energetic trap distribution (determined earlier) and assuming a simple analytical form of the spatial trap distribution with one or several parameters. The values of these parameters may be obtained by comparing the calculated TSC curves with the experimental ones.

## 5. Concluding remarks

In the present work we have discussed the influence of spatial non-homogeneity of trap distribution on TSC in the case of surface generation of free carriers. We have shown that for both non-dispersive and dispersive transport the initial increase of TSC is strongly dependent on the spatial distribution of traps. In particular, distinct polarity effects have been predicted. The analytical results have been found to agree satisfactorily with the results of Monte Carlo simulation of non-isothermal carrier transport for all the model spatial and energetic trap distributions considered, which allowed us to propose methods for determining the spatial trap distribution on the basis of the measured TSC.

The second physically important case is the bulk generation of charge carriers in the layer. We do not see at present how to solve the transport equations with such an initial condition for arbitrary shape function  $S(x)$ . The expressions for TSC may be found only

for some given *a priori* relatively simple functions  $S(x)$ . Our Monte Carlo simulations of TSC in the case of bulk generation show qualitatively similar, but much less distinct, dependences of the peak shapes on spatial non-homogeneity in trap concentration.

### Acknowledgment

The work has been partially sponsored by CPBP 0108E.

### References

- Marshall J M 1977 *Phil. Mag.* **36** 959  
— 1983 *Rep. Prog. Phys.* **46** 1235  
Noolandi J 1977a *Phys. Rev. B* **16** 4466  
— 1977b *Phys. Rev. B* **16** 4474  
Pfister G and Scher H 1978 *Adv. Phys.* **27** 747  
Plans J, Baltá Calleja F J, Zieliński M and Kryszewski M 1983 *Phil. Mag.* **B 23** 289  
Plans J, Zieliński M and Kryszewski M 1981 *Phys. Rev. B* **23** 6557  
Ramo S 1939 *Proc. IRE* **27** 584  
Rybicki J and Chybicki M 1988 *J. Phys. C: Solid State Phys.* **21** 3077  
— 1989 *J. Phys.: Condens. Matter* **1** 4623  
Samoć M and Samoć A 1980 *Phys. Status Solidi a* **57** 667  
Samoć M and Zboiński Z 1978 *Phys. Status Solidi a* **46** 251  
Scher H and Montroll E W 1975 *Phys. Rev. B* **12** 2455  
Schmidlin F W 1977 *Phys. Rev. B* **16** 2362  
Schrader S and Kryszewski M 1985 *Phys. Status Solidi a* **91** 243  
Tomaszewicz W 1985 *Phil. Mag.* **B 52** 881  
— 1988 *Proc. ISE* **6** 571  
Tomaszewicz W and Jachym B 1984 *J. Non-Cryst. Solids* **65** 193